

Finding a 61.0-day orbital period for the HMXB 4U 1036–56 with the Swift-BAT monitoring.

G. Cusumano¹, A. Segreto¹, V. La Parola¹, N. Masetti², A. D’Ai³, G. Tagliaferri⁴

¹INAF - Istituto di Astrofisica Spaziale e Fisica Cosmica, Via U. La Malfa 153, I-90146 Palermo, Italy

²INAF - Istituto di Astrofisica Spaziale e Fisica Cosmica di Bologna, via Gobetti 101, 40129, Bologna, Italy

³Dipartimento di Fisica e Chimica, Università di Palermo, via Archirafi 36, 90123, Palermo, Italy

⁴INAF - Brera Astronomical Observatory, via Bianchi 46, 23807, Merate (LC), Italy

ABSTRACT

Since November 2004, the Burst Alert Telescope on board Swift is producing a monitoring of the entire sky in the 15–150 keV band, recording the timing and spectral behavior of the detected sources. Here we study the properties of the HMXB 4U 1036–56 using both the BAT survey data and those from a Swift-XRT observation. A folding analysis performed on the BAT light curve of the first 100 months of survey unveils a periodic modulation with a period of ~ 61.0 days, tied to the presence in the BAT light curve of several intensity enhancements lasting $\sim 1/4$ of P_0 . We explain this modulation as the orbital period of the binary system. The position of 4U 1036–56 on the Corbet diagram, the derived semi-major orbit axis ($\approx 180 R_\odot$), and the bulk of the source emission observed in a limited portion of the orbit are consistent with a Be companion star. The broad band 0.2–150 keV spectrum is well modeled with a flat absorbed power law with a **cut-off at ~ 16 keV**. Finally, we explore the possible association of 4U 1036–56 with the γ -ray source AGL J1037–5808, finding that the BAT light curve does not show any correlation with the γ -ray outburst observed in November 2012.

Key words: X-rays: binaries – X-rays: individual: 4U 1036–56.
Facility: *Swift*

1 INTRODUCTION

The identification of the orbital period of a binary system is an essential step for deriving the geometry of the system and, as a consequence, for investigating the physical mechanism responsible for the spectral and temporal properties of the source. However, the discovery of such modulations may become a challenging task for very long periodicities, requiring long and continuous monitoring. For sources with strong absorption this monitoring is efficient only in the hard X-ray regime where the circumstellar material is transparent to the emission, while it blocks most of the emission in the soft X-ray band. The long-term temporal monitoring carried on by the Burst Alert Telescope (BAT, Barthelmy et al. 2005) on board of the Swift observatory (Gehrels et al. 2004) has been fulfilling this task (e.g. Corbet & Krimm 2009; Corbet et al. 2010a,b; Cusumano et al. 2010; La Parola et al. 2010; D’Ai et al. 2011).

In this Letter we analyze the dataset collected by Swift on 4U 1036–56. This source was first detected by UHURU (Forman et al. 1978) and its transient behavior was first observed by Ariel V in 1974 (Warwick et al. 1981), that recorded an outburst episode with a flux increase of a factor of 2.4 higher than the average UHURU flux. Since then, 4U 1036–56 was observed by several X-ray telescopes, at different luminosity levels ranging between 10^{34} and 3×10^{35} erg s⁻¹ (see La Palombara et al. 2009 and ref-

erences therein). RXTE data revealed a pulsed emission with a period of 860 ± 2 s (Reig & Roche 1999). Based on a pointed ROSAT PSPC observation Motch et al. (1997) identified the optical counterpart to be the B0 III-Ve star LS 1698, at a distance of ~ 5 kpc. BAT detected a hard X-ray outburst from 4U 1036–56 with a peak flux of ~ 30 mCrab on February 2012 (Krimm et al. 2012). This activated a Swift-XRT target-of-opportunity observation. The XRT spectrum was modeled with an absorbed flat power law with photon index ~ 0.6 . Li et al. (2012) report timing and spectral analysis of 4U 1036–56 with INTEGRAL (Winkler et al. 2003) and Swift data. They report an outburst detected in February 2007 with a significance ~ 30 and ~ 10 standard deviations in ISGRI and JEM-X, respectively. Their broad band spectrum can be described by an absorbed power-law (with photon index ~ 1.1) modified by a cut-off at ~ 26 keV. Using the Swift-XRT observation, they confirm the pulsed modulation reported by Reig & Roche (1999). They also discuss the possibility that 4U 1036–56 is associated to the MeV source AGL J1037–5708 (as suggested by Bulgarelli et al. 2010 upon the detection of the AGILE source). Using theoretical considerations based on the leptonic model for γ -ray emission, they do not rule out this possibility.

This Letter is organized as follows. Section 2 describes the BAT and XRT data reduction. Section 3 reports on the timing analysis.

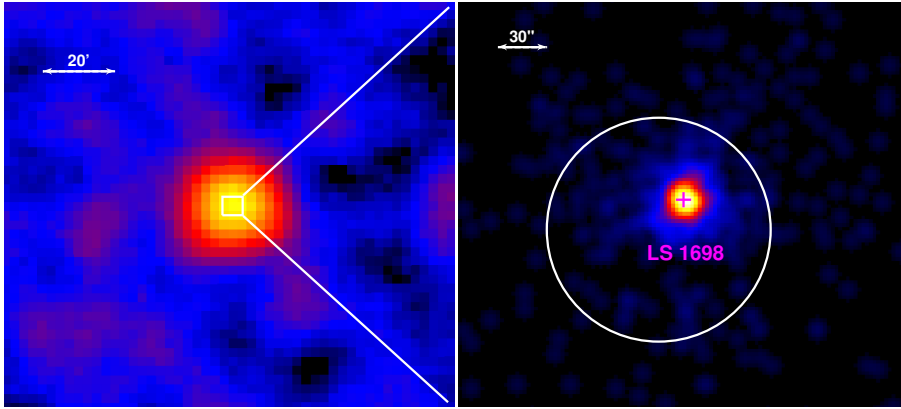


Figure 1. Left panel: 15–60 keV significance map centered on 4U 1036–56. The box represents the sky area in the right panel. Right panel: 0.2–10 keV XRT image; the circle represents the 95% BAT error box of 1.16'. The position of the optical counterpart (LS 1698) suggested by Motch et al. (1997) is marked with a cross.

Sect. 4 describes the broad band spectral analysis. In Sect. 5 we briefly discuss our results.

2 DATA REDUCTION

The survey data collected with BAT between November 2004 and March 2013 were retrieved from the HEASARC public archive¹ and processed using a software dedicated to the analysis of the data from coded mask telescopes (Segreto et al. 2010). The source is detected with a significance of 26.8 standard deviations in the 15–60 keV energy band, where its signal is optimized: Fig. 1 (left panel) shows the significance map of the sky region around 4U 1036–56 in this energy band. The significance in the 15–150 keV band is 23.9 standard deviations. The 15–60 keV light curve was extracted in 49493 bins with a variable time length ranging between 50 s and 6317 s and a constant pointing direction within each bin. The central time of each bin was corrected to the Solar System barycentre (SSB) using the task EARTH2SUN and the JPL DE-200 ephemeris (Standish 1982). The background subtracted spectrum was extracted in eight energy channels and analyzed using the BAT redistribution matrix available in the Swift calibration database².

4U 1036–56 was observed once (ObsID 00032288001) with Swift-XRT on 2012 February 17 for 3 ksec in photon counting observing mode (Hill et al. 2004). The data were processed using the FTOOLS package with standard procedures (XRTPIPELINE v.0.12.4), filtering and screening criteria, with standard grade filtering 0–12.

A first inspection of the light curve shows high variability, with a maximum count rate of 1.2 c/s, indicating the need for a pile-up correction³. Selecting only the time intervals where the source intensity exceeds 0.5 c/s, we have compared the source Point Spread function (PSF) with the expected PSF shape (Moretti et al. 2005), finding that a circular region with **4 pixels radius** (centered at the source position) must be excluded to avoid pile-up. Therefore, the source spectrum and light curve were extracted from an

annular region of **4 and 30 pixels internal and external radii** respectively, centered on the source centroid as determined with the task XRTCENTROID ($RA_{J2000}=10\text{h }37\text{m }35.25\text{s}$, $Dec_{J2000}=-56^\circ 47' 56.3''$, with 3.6'' uncertainty at 90% confidence level). The background **for the lightcurve and spectral analysis** was extracted from an annular region with inner and outer radii of 40 and 70 pixels, respectively. This annular region is far enough to avoid the contamination from the PSF wings of 4U 1036–56 and does not contain any field source. **The source event arrival times were converted to the Solar System barycenter using the task BARYCORR; the lightcurve was corrected for PSF and vignetting using the task XRTLCCORR.** The XRT ancillary response file generated with XRTMKARF accounts for PSF and vignetting correction; we used the spectral redistribution matrix v013 available in the Swift calibration database. The spectral analysis was performed using XSPEC v.12.5, after grouping the spectrum with a minimum of 20 counts per channel to allow the use of χ^2 statistics.

We note that the X–ray coordinates of 4U 1036–56 determined with XRT are formally inconsistent with those ($RA_{J2000} = 10\text{h }37\text{m }35.5\text{s}$, $Dec_{J2000} = -56^\circ 48' 11''$) of the optical counterpart LS 1698 (Stephenson & Sanduleak 1971) which are available e.g. from the CDS⁴ Portal, the star being about 20'' from the X–ray centroid, thus well outside the XRT error circle. However, an inspection of this sky region in the DSS-II-Red Sky Survey⁵ shows that no object is present at the CDS coordinates of LS 1698. Moreover, a bright optical object is instead present in the DSS within the XRT error circle, and this is the same object proposed by Motch et al. (1997, see their Fig. 14) as the optical counterpart of 4U 1036–56. Regrettably, Motch et al. (1997) did not report precise coordinates for LS 1698; we thus complete this information here by extracting it from the 2MASS archive, which has a precision of 0'.1 on both RA and Dec (Skrutskie et al. 2006). According to this archive, the coordinates (J2000) of LS 1698 are $RA_{J2000} = 10\text{h }37\text{m }35.32\text{s}$, $Dec_{J2000} = -56^\circ 47' 55.8''$, at 0'.7 from the XRT error circle centroid, thus well within it. Figure 1 (right panel) shows the XRT image of 4U 1036–56, with the 95% BAT error circle of 1.16' superimposed, and the position of the optical counterpart.

¹ <http://heasarc.gsfc.nasa.gov/docs/archive.html>

² <http://swift.gsfc.nasa.gov/docs/heasarc/caldb/swift/>

³ see e.g. <http://www.swift.ac.uk/analysis/xrt/pileup.php>

⁴ <http://cdsportal.u-strasbg.fr>

⁵ <http://archive.eso.org/dss/dss>

[h]

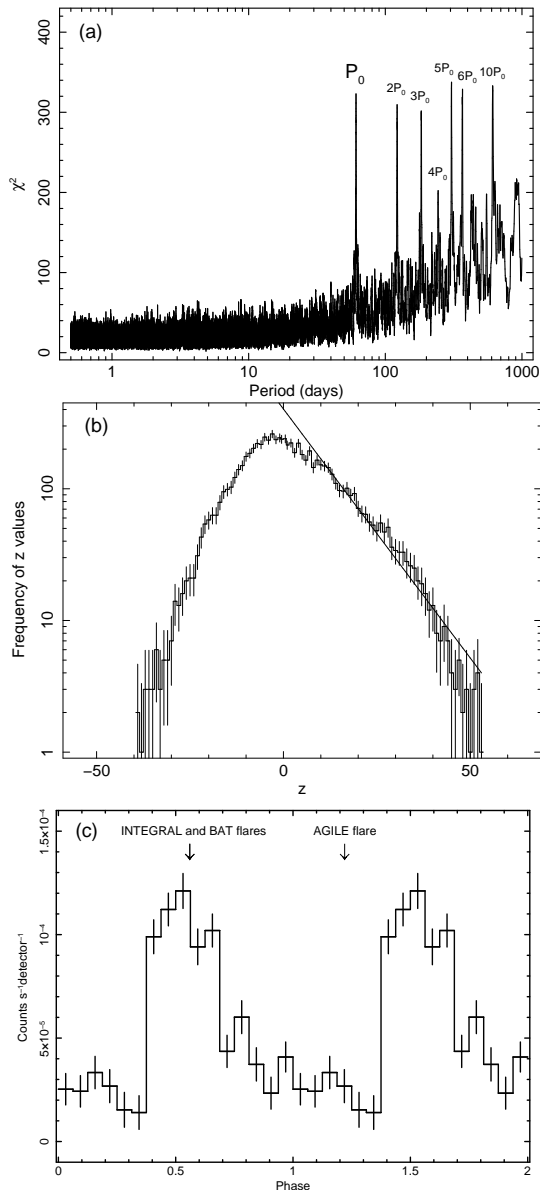


Figure 2. a: Periodogram of *Swift*-BAT (15–60 keV) data for 4U 1036–56. b: Distribution of the z values derived from the χ^2 periodogram (see Section 3). The positive tail beyond $z=10$ is modeled with an exponential function. c: Light curve folded at a period $P_0=61.0$ days, with 16 phase bins. The INTEGRAL (Li et al. 2012) and BAT (Krimm et al. 2012) flares at phase 0.55 and 0.57 respectively, together with the AGL J1037-5708 flare (Bulgarelli et al. 2010) at phase 0.22, are marked with arrows.

3 TIMING ANALYSIS

We performed a timing analysis searching for long term periodic modulations in the 15–60 keV BAT light curve of 4U 1036–56. We applied a folding algorithm to the baricentered arrival times searching in the **0.5–1000 days** time range with a step of $P^2/(N \Delta T)$, where P is the trial period, $N = 16$ is the number of profile phase bins and $\Delta T = 262$ Ms is the data time span. The average rate in each phase bin was evaluated by weighting the rates by the inverse square of the corresponding statistical errors (see

also Cusumano et al. 2010). This is appropriate when dealing with a large span of rate errors and/or with background dominated data such as those from coded mask telescopes.

Figure 2 (a) shows the periodogram with several features emerging. A very prominent one, with a χ^2 value of ~ 323 , is at $P_0 = 61.0 \pm 0.2$ d, where the period and its error ΔP_0 are the centroid of the peak and the standard deviation obtained from a Gaussian fit to the χ^2 feature at P_0 ; other significant features at higher periods correspond to multiples of P_0 ($2P_0$ to $10P_0$).

The long term variability of the source causes the distribution of χ^2 in Figure 2 (a) to deviate strongly both in average and in fluctuation amplitude from the behavior expected for a white noise (average $\chi^2 = N - 1$) where the signal is dominated by statistical variations. As a consequence the χ^2 statistics cannot be applied and the significance for the presence of a feature has to be evaluated with different methodologies. For this purpose we applied the procedure described below in a few steps:

(1) - The significance of any feature needs to be evaluated with respect to the average level of the periodogram. Thus we fit the periodogram with a second order polynomial that describes the trend of the χ^2 values in the periodogram. The best fit function was then subtracted from the χ^2 to obtain a flattened periodogram (hereafter, z). The value of z corresponding to P_0 is ~ 279 .

(2) - Figure 2 (b) shows the histogram of the z values in the period range between 20 and 100 days (where the periodogram is characterized by a noise level quite consistent with the noise level at P_0), excluding the values in the interval $\pm 3\Delta P_0$ around P_0 . Its positive tail (beyond $z=10$) can be modeled with an exponential function, and its integral Σ between 279 and infinity (normalized to the total area below the distribution) represents the probability of chance occurrence of a z equal to or larger than 279. The area below the histogram was evaluated summing the contribution of each single bin from its left boundary up to $z=10$ and integrating the best-fit exponential function beyond $z=10$. The probability of chance occurrence for $z \geq 279$ is $\Sigma = 1.7 \times 10^{-11}$ and corresponds to ~ 6 Gaussian standard deviations for the significance of the feature at P_0 . The light curve profile (Fig. 2, c) folded at P_0 with $T_{\text{epoch}} = 54841.199$ MJD, is characterized by a roughly squared shaped peak over a low intensity plateau.

Figure 3 shows the 15–60 keV BAT light curve of 4U 1036–56 sampled with a bin time of $P_0/4 = 15.25$ d. The vertical shaded area are in phase with the peak in Figure 2c (phase interval 0.375–0.6875). The light curve shows the presence of many flux enhancement, most of which are coincident with the shaded bars.

The *Swift*-XRT observation was performed as a follow up of the BAT flare (Krimm et al. 2012) and it is at orbital phase 0.58 in Fig. 2(c). It is composed of two snapshots lasting ~ 2200 s and 800 s respectively, with an average pile-up corrected count rate of 0.6 count s^{-1} . A light curve binned at intervals of 50 s (Fig. 4) shows a variability within a factor of 10, with a modulation (~ 3 cycles) roughly consistent with the periodicity reported by Reig & Roche (1999).

4 SPECTRAL ANALYSIS

Since the XRT observation was performed during a flare, which in turn corresponds to the phase interval where several other intensity enhancements have been observed (see Figure 3), the broad band spectral analysis was performed coupling the soft X-ray spectrum

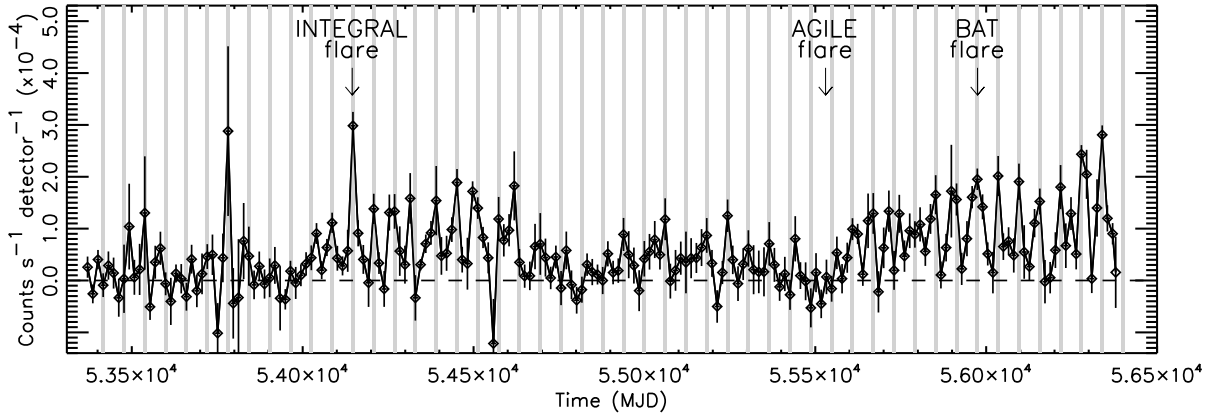


Figure 3. 15–60 keV BAT light curve. Each bin represents a time interval of $P_0/4 = 15.25$ d. The vertical shaded bars correspond to phase 0.375–0.6875 in Figure 2c. The epochs of the INTEGRAL (Li et al. 2012) and BAT (Krimm et al. 2012) flares, together with the epoch of the AGL J1037-5708 flare (Bulgarelli et al. 2010) are marked with arrows.

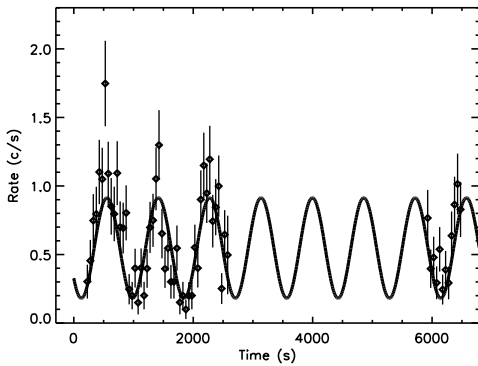


Figure 4. 0.2–10 keV XRT light curve. Each bin represents a time interval of 50 s. The solid line represents a sinusoidal modulation with the pulse period of 860 s reported by Reig & Roche (1999).

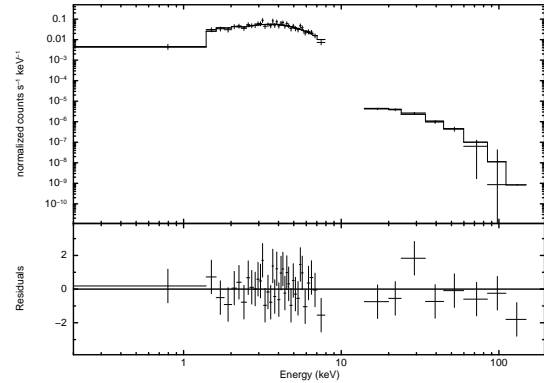


Figure 5. 4U1036-56 broad band (0.2–150 keV) spectrum. **Top panel:** XRT and BAT data and best fit `phabs*(cutoffpl)` model. **Bottom panel:** Residuals in unit of standard deviations.

and the Swift-BAT hard X-ray spectrum selected at this phase interval (0.375–0.6875).

The broad band 0.2–150 keV spectral analysis was performed introducing a multiplicative constant (C_{BAT}) in the model to take into account both for the intercalibration systematics in the XRT and BAT responses and for the non simultaneity of the data. We tried to fit the spectra with an absorbed power law model `phabs*(powerlaw)` that resulted unsatisfactory to describe the data ($\chi^2=91.2$, 41 degrees of freedom [d.o.f.]). The fit residuals clearly indicated a significant steepening in the BAT energy range. The spectrum indeed results well fitted adopting the model `phabs*(cutoffpl)` with a photon index $\Gamma \sim 0.6$ and a cut-off energy $E_{cut} \sim 16$ keV, with a $\chi^2 = 32.5$, for 40 dof. The F-test for one additional parameter yields a probability of chance improvement of 1.7×10^{-10} with respect to the absorbed power-law model. **We observe that the cutoff energy is close to the gap between the XRT and the BAT energy bands; therefore its position could be affected by residual intercalibration systematics between the two instruments.** Figure 5 (bottom panel) shows no significant residual pattern between data and model. Table 1 reports the best fit parameters (quoted errors are given at 90% confidence level for a single parameter). **The multiplicative con-**

stant (C_{BAT}) is marginally consistent with the ratio between the average count rate in the BAT spectrum and the count rate observed by BAT at the time of the XRT observation.

5 DISCUSSION

We investigated the timing and spectral properties of the HMXB 4U 1036–56 exploiting the Swift data recorded by the BAT and the XRT telescopes. The timing analysis on the 100-month BAT survey light curve unveiled a periodic modulation with a period of $P_0 = 61.0 \pm 0.2$ days. Such long periodicities are typically associated with the orbit of binary systems. The profile of the light curve folded at P_0 shows a roughly rectangular shape over a plateau of low intensity emission.

The source can be located on the Corbet diagram (Corbet 1986), as both its spin and orbital periods (P_{spin} , P_{orb}) are known. Figure 6 reports the pairs of P_{spin} and P_{orb} for the HMXBs listed in Liu et al. (2006), and for the HMXBs discovered more recently by INTEGRAL⁶. 4U 1036–56 lays at the boundary of the Be tran-

⁶ <http://irfu.cea.fr/Sap/IGR-Sources/>

| Parameter | Best fit value | Units |
|--------------------------|-------------------------------------|--|
| N_{H} | $2.2^{+0.8}_{-0.6} \times 10^{22}$ | cm^{-2} |
| Γ | $0.6^{+0.3}_{-0.3}$ | |
| E_{cut} | 16^{+5}_{-3} | keV |
| N | $4.3^{+2.9}_{-1.6} \times 10^{-3}$ | $\text{ph keV}^{-1} \text{cm}^{-2} \text{s}^{-1}$ at 1 keV |
| C_{BAT} | $0.18^{+0.08}_{-0.05}$ | |
| $F_{0.2-10 \text{ keV}}$ | $8.7^{+0.7}_{-0.7} \times 10^{-11}$ | $\text{erg s}^{-1} \text{cm}^{-2}$ |
| $F_{15-150 \text{ keV}}$ | $3.2^{+0.2}_{-0.3} \times 10^{-11}$ | $\text{erg s}^{-1} \text{cm}^{-2}$ |
| χ^2 | 32.5 (40 dof) | |

Table 1. Best fit spectral parameters. The BAT spectra is selected in the phase interval 0.375-0.6875 in Fig. 2 (c). We report unabsorbed fluxes for the characteristic XRT (0.2–10 keV) and BAT (15–150 keV) energy bands. C_{BAT} is the constant factor to be multiplied to the model in the BAT energy range in order to match the BAT data.

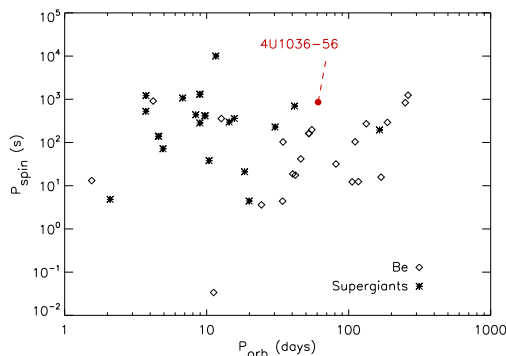


Figure 6. Corbet diagram for HMXBs with known spin and orbital period. Diamond and star points represent the Be and supergiant systems, respectively. The red filled circle marks the position of 4U 1036-56.

sients region, in agreement with the classification of its companion star.

Knowing the orbital period, we can use the third Kepler’s law to derive the semi-major axis of the binary system. Assuming that $M_X = 1.4 M_\odot$ is the mass of the neutron star and $M_* = 17.5 - 20 M_\odot$ is the mass range for the spectral type of the companion star (Lang 1992), we have:

$$a = (GP_0^2 (M_* + M_X)/4\pi^2)^{1/3} \simeq 174 - 181 R_\odot \quad (1)$$

Considering that the radius of the companion star is $R_* = 7.4 - 15 R_\odot$ (Lang 1992), **the semi-major axis length corresponds to $\sim 12 - 23.5 R_*$** . This wide orbital separation is common among HMXB with Be star as companion.

We analyzed the broad-band (0.2–150 keV) spectrum of 4U 1036–56 using the XRT pointed observation data in the soft X-ray band and the BAT survey data selected in the 0.375–0.6875 phase interval. The spectrum is well modeled with a flat ($\Gamma \sim 0.6$) absorbed powerlaw with a cutoff at ~ 16 keV. The column density is $\sim 2.2 \times 10^{22} \text{cm}^{-2}$, which is a factor of ~ 2 larger than the maximum Galactic value in the direction of the source ($9.1 \times 10^{21} \text{cm}^{-2}$ Dickey & Lockman 1990). This suggests an additional intrinsic absorption in the environment of the binary system.

Li et al. (2012) discuss the possibility that 4U 1036–56 is associated to the unidentified source AGL J1037-5708, that was detected in November 2012 during an outburst above 100 MeV

(Bulgarelli et al. 2010). The association was initially suggested because of the spatial coincidence of the two sources. Figure 3 shows the epoch of the INTEGRAL (Li et al. 2012) and BAT (Krimm et al. 2012) flares, together with the epoch of the AGL J1037-5708 flare (Bulgarelli et al. 2010). A simultaneous flare in the MeV and in the hard X-ray energy ranges would be a strong evidence that the two sources are indeed associated. However, while the presence of **many peaks** can be observed in the BAT light curve, the epoch of the MeV burst does not correspond to any significant intensity enhancement. Moreover we observe that while the BAT and the INTEGRAL flare happen at a phase consistent with the maximum of the folded profile (Figure 2c), the MeV flare is at a phase of minimum intensity. On the other hand, it is not ensured that a MeV flare would automatically corresponds to a hard X-ray flare.

ACKNOWLEDGMENTS

This work has been supported by ASI grant I/011/07/0.

REFERENCES

- Barthelmy, S. D., et al. 2005, *Space Science Reviews*, 120, 143
- Bulgarelli, A., Gianotti, F., Trifoglio, M., et al. 2010, *The Astronomer’s Telegram*, 3059, 1
- Corbet, R. H. D., & Krimm, H. A. 2009, *The Astronomer’s Telegram*, 2008, 1
- Corbet, R. H. D., Krimm, H. A., & Skinner, G. K. 2010, *The Astronomer’s Telegram*, 2559, 1
- Corbet, R. H. D., Krimm, H. A., Barthelmy, S. D., et al. 2010, *The Astronomer’s Telegram*, 2570, 1
- Corbet, R. H. D. 1986, *MNRAS*, 220, 1047
- Cusumano, G., La Parola, V., Romano, P., et al. 2010, *MNRAS*, 406, L16
- D’Ai, A., La Parola, V., Cusumano, G., et al. 2011, *A&A*, 529, A30
- Dickey, J. M., & Lockman, F. J. 1990, *ARA&A*, 28, 215
- Forman, W., Jones, C., Cominsky, L., et al. 1978, *ApJS*, 38, 357
- Gehrels, N., et al. 2004, *ApJ*, 611, 1005
- Hill, J. E., Burrows, D. N., Nousek, J. A., et al. 2004, *SPIE*, 5165, 217
- Krimm, H. A., Kennea, J. A., Holland, S. T., et al. 2012, *The Astronomer’s Telegram*, 3936, 1
- Lang, K. R. 1992, *Astrophysical Data I. Planets and Stars*, X, 937 pp. 33 figs.. Springer-Verlag Berlin Heidelberg New York
- La Palombara, N., Sidoli, L., Esposito, P., Tiengo, A., & Mereghetti, S. 2009, *A&A*, 505, 947
- La Parola, V., Cusumano, G., Romano, P., et al. 2010, *MNRAS*, 405, L66
- Li, J., Torres, D. F., Zhang, S., et al. 2012, *ApJ*, 761, 49
- Liu, Q. Z., van Paradijs, J., & van den Heuvel, E. P. J. 2006, *A&A*, 455, 1165
- Moretti, A., Campana, S., Mineo, T., et al. 2005, *SPIE*, 5898, 360
- Motch, C., Haberl, F., Dennerl, K., Pakull, M., & Janot-Pacheco, E. 1997, *A&A*, 323, 853
- Reig, P., & Roche, P. 1999, *MNRAS*, 306, 100
- Segreto, A., Cusumano, G., Ferrigno, C., La Parola, V., Mangano, V., Mineo, T., & Romano, P. 2010, *A&A*, 510, A47
- Skrutskie, M. F., Cutri, R. M., Stiening, R., et al. 2006, *The Astronomical Journal*, 131, 1163

- Standish, E. M., Jr. 1982, *A&A*, 114, 297
Stephenson, C. B., & Sanduleak, N. 1971, *Publications of the Warner & Swasey Observatory*, 1, 1
Warwick, R. S., Marshall, N., Fraser, G. W., et al. 1981, *MNRAS*, 197, 865
Winkler, C., Courvoisier, T. J.-L., Di Cocco, G., et al. 2003, *A&A*, 411, L1

This paper has been typeset from a $\text{\TeX}/\text{\LaTeX}$ file prepared by the author.